

## EXPERIMENTAL STUDY

# Could pyrimidine derivative be effective against Omicron of SARS-CoV-2?

KARATAS Halis<sup>1</sup>, TUZUN Burak<sup>2</sup>, KOKBUDAK Zulbiye<sup>1</sup>

Sivas Cumhuriyet University, Plant and Animal Production Department, Technical Sciences Vocational School of Sivas, Sivas, Turkey. [theburaktuzun@yahoo.com](mailto:theburaktuzun@yahoo.com)

**ABSTRACT**

**BACKGROUND:** A pyrimidine based Schiff base was examined in this report. Structural and spectral characterizations were done with Gaussian software. Active sites of the compound were determined using molecular electrostatic potential (MEP) maps.

**AIM:** We focused to determine whether pyrimidine based Schiff base would be an inhibitor against Omicron of SARS-CoV-2 in silico.

**RESULTS AND CONCLUSION:** As one of the perils the world has seen lately, omicron of SARS-CoV-2, is a complication to be solved. For the sake of that, anti-viral properties of studied pyrimidine based Schiff base compound were investigated with molecular docking calculations. It was found that the quantitative values of the calculated parameters were in the applicable ranges. In accordance with these results, it will be an important guide for future in vitro and in vivo analysis (Tab. 3, Fig. 7, Ref. 70). Text in PDF [www.elis.sk](http://www.elis.sk)

**KEY WORDS:** Pyrimidine, Schiff base, omicron of SARS-CoV-2, DFT, Molecular docking, ADME/T.

**Introduction**

As a member of coronavirus strain, severe acute respiratory syndrome coronavirus 2 (SARS-CoV-2) (1), which causes respiratory disorder called coronavirus disease 2019 (COVID-19), is responsible for the current COVID-19 pandemic. The virus heretofore had different names such as human coronavirus 2019 (HCoV-19) (2–4) and 2019 novel coronavirus (2019-nCoV) (5–8). After the first diagnosis in Wuhan, China, December 2019, the World Health Organization (WHO) announced the disease as a pandemic on 11 March 2020 (9).

Human to human contagion of the virus was validated in January 2020 (10). Transmission was expected to appear particularly by respiratory droplets from coughs and sneezes (11–13). Whether the virus shows pathogenic properties before or after the spread is unclear. Bats are considered a prospective natural source of SARS-CoV-2, however, dissimilarity between bat virus and SARS-CoV-2 indicate that humans may have been infected by an intermediate host (14).

Many conspicuous variants of SARS-CoV-2 occurred in late 2020. Currently, there are five variants affirmed by WHO, which are the alpha, beta, gamma, delta and omicron variants. In all variants, transmissibility, virulence and antigenicity of the virus changed (15).

Since the beginning of the pandemic, there have been nearly 320 million people affected by Covid-19 including more than 5 million deaths, as reported by World Health Organization (WHO) (16). The academic recognition of SARS-CoV-2, in respect of the public health, financial and communal influences of the COVID-19 pandemic and how it spreads, have continuously evolved. Thanks to the unceasing endeavors of many scientists, several drugs have been discovered and they have gradually controlled the transmission of the epidemic (17–21).

Drug chemistry approaches intent to ameliorate advanced candidates to evolve in the drug industry, in which a vast diversity of instruments involving various related disciplines are implemented. Two of the predominantly used methods to synthesize prospective drug candidates are DFT and molecular docking calculations.

When theoretical calculations are done before experimental procedures, it provides important information in the determination of the active sites of the molecules (22–24). With theoretical calculations, it is possible to synthesize more effective and more active molecules. In addition, it is possible to compare the activities of molecules with the theoretical calculations done for the SARS-CoV-2 virus, one of the most important diseases of today (25, 26). Furthermore, ADME/T (absorption, distribution, metabolism, excretion and toxicity) calculations were performed in order for the molecule to determine its usability as a drug candidate.

<sup>1</sup>Erciyes University, Faculty of Sciences, Department of Chemistry, Kayseri, Turkey, and <sup>2</sup>Sivas Cumhuriyet University, Plant and Animal Production Department, Technical Sciences Vocational School of Sivas, Sivas, Turkey

**Address for correspondence:** TUZUN Burak, Sivas Cumhuriyet University, Plant and Animal Production Department, Technical Sciences Vocational School of Sivas, 58140, Sivas, Turkey.

**Acknowledgements:** This work is supported by the Scientific Research Project Fund of Sivas Cumhuriyet University under project number RGD-020. This research was made possible by the TUBITAK ULAKBIM, High Performance and Grid Computing Center (TR-Grid e-Infrastructure).

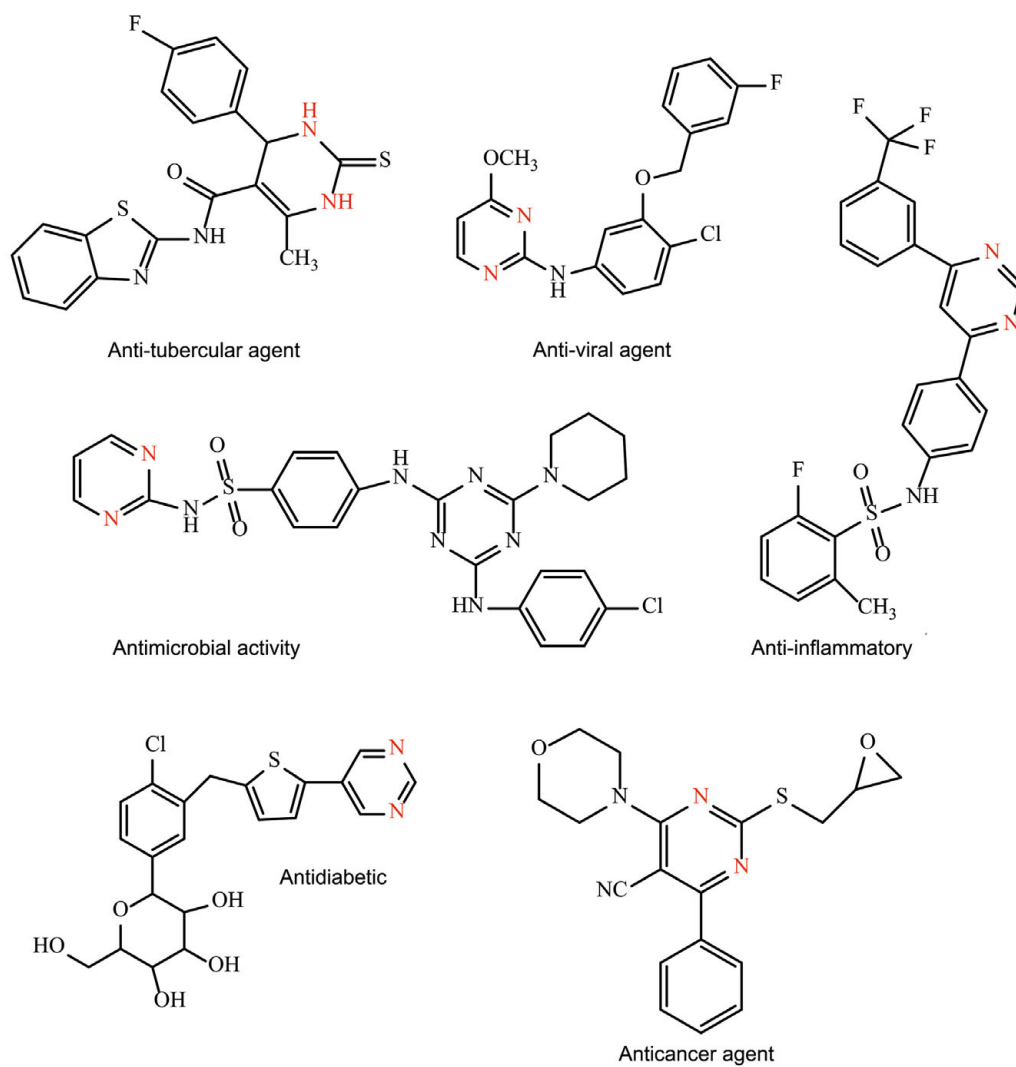


Fig. 1. Some pyrimidine based biologically active molecules.

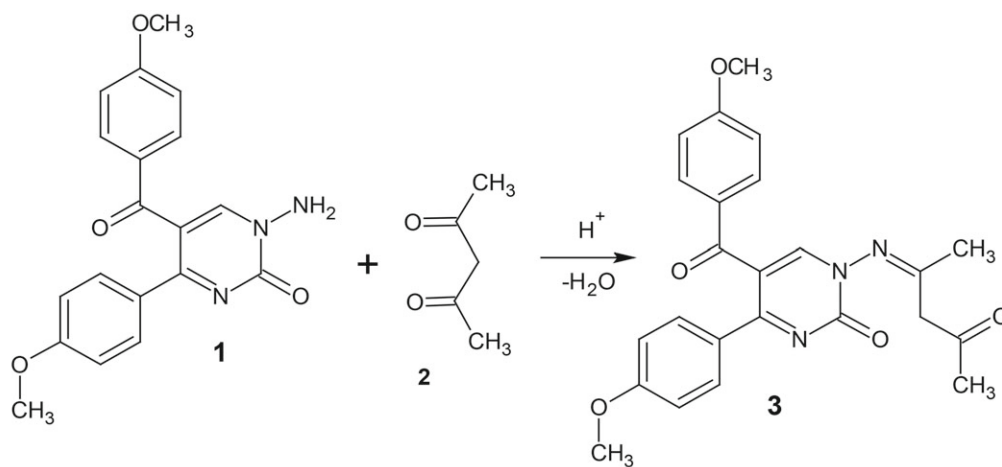


Fig. 2. Synthesis scheme for the compound 3.

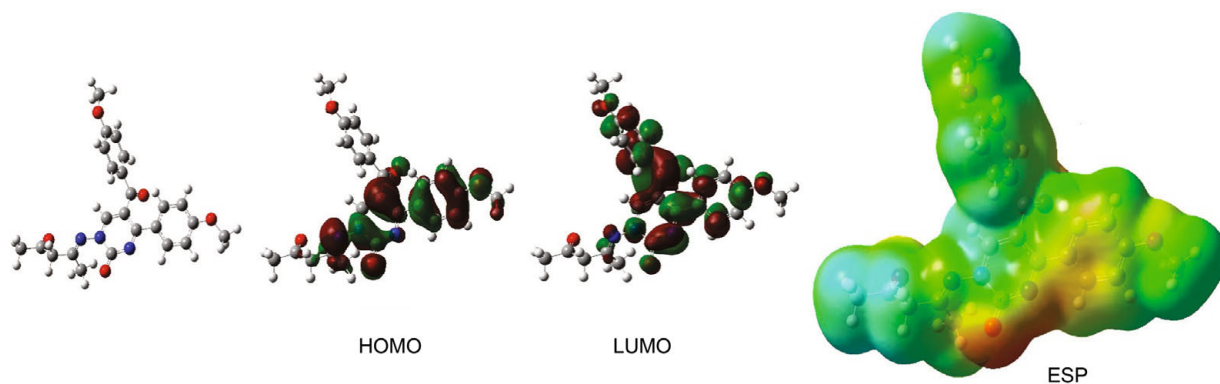
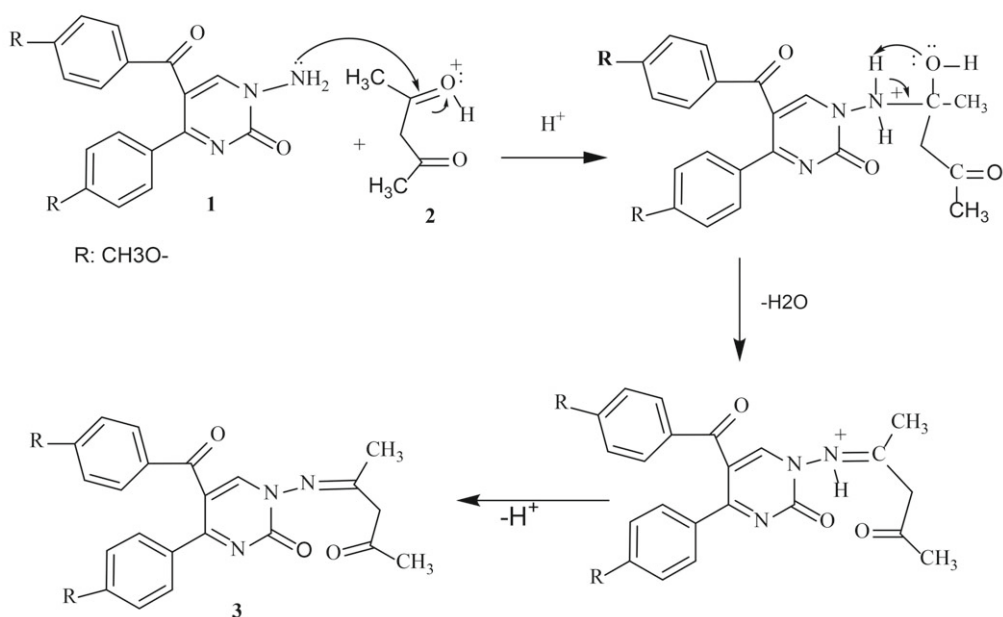
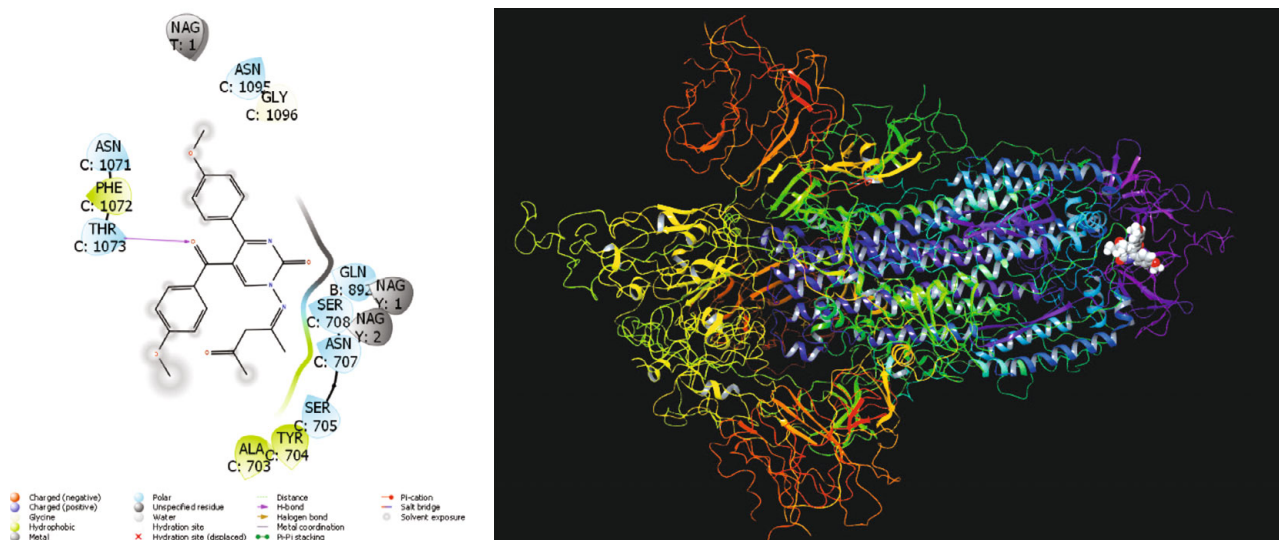


Fig. 4. Representations of optimized structure, HOMO, LUMO and ESP (electrostatic potential) of molecule.



Tab. 1. The calculated quantum chemical parameters of molecules.

	EHOMO	ELUMO	I	A	ΔE	η	μ	χ	PI	ω	ε	dipol	Energy
B3LYP/3-21g LEVEL	-5.9316	-1.9138	5.9316	1.9138	4.0178	2.0089	0.4978	3.9227	-3.9227	3.8298	0.2611	8.1180	-39736.2850
B3LYP/6-31g LEVEL	-6.0165	-2.0322	6.0165	2.0322	3.9843	1.9922	0.5020	4.0243	-4.0243	4.0647	0.2460	5.0733	-39944.6560
B3LYP/SDD LEVEL	-6.2151	-2.3522	6.2151	2.3522	3.8630	1.9315	0.5177	4.2837	-4.2837	4.7502	0.2105	7.7291	-39950.0308
HF/3-21g LEVEL	-8.3376	2.0885	8.3376	-2.0885	10.4261	5.2131	0.1918	3.1246	-3.1246	0.9364	1.0679	6.5414	-39491.8913
HF/6-31g LEVEL	-8.3550	1.8297	8.3550	-1.8297	10.1848	5.0924	0.1964	3.2627	-3.2627	1.0452	0.9568	5.2139	-39696.4515
HF/SDD LEVEL	-5.0124	1.2523	5.0124	-1.2523	6.2647	3.1323	0.3193	1.8800	-1.8800	0.5642	1.7724	7.0242	-39701.6188
M062X/3-21g LEVEL	-7.3893	-1.0623	7.3893	1.0623	6.3270	3.1635	0.3161	4.2258	-4.2258	2.8225	0.3543	5.1812	-39719.3553
M062X/6-31g LEVEL	-7.2628	-1.0131	7.2628	1.0131	6.2497	3.1248	0.3200	4.1379	-4.1379	2.7397	0.3650	7.7028	-39928.3917
M062X/SDD LEVEL	-7.6290	-1.5266	7.6290	1.5266	6.1025	3.0512	0.3277	4.5778	-4.5778	3.4341	0.2912	7.4103	-39934.4641

The calculations of the molecule were done with 3 different methods and in 3 different basis sets. It was investigated how the parameters of the molecules were affected by the calculations made this way.

N-aminopyrimidine-2-one derivatives appear to be an important starting compound in synthetic organic chemistry. In recent years, the reactions of aminopyrimidine-2-one derivatives with anhydrides (27), isothiocyanate, isocyanate (28), carbonyl compounds (29), acyl chlorides (30), benzaldehydes derivatives (Schiff bases) and transition metal complexes(31–34) have been reported in different solvents and at various temperatures. Nowadays, theoretical and experimental comparison of N-aminopyrimidine-2-one derivatives has become popular (35–37). Moreover, these compounds have biological and pharmacological properties. Prior studies have shown that N-aminopyrimidine-2-one derivatives have antitubercular, antiviral, anti-inflammatory, antidiabetic, antimicrobial and anticancer properties (38–44). Some pyrimidine based biologically active molecules are shown in Figure 1.

In this study, 1-amino-5-(4-methoxybenzoyl)-4-(4-methoxyphenyl)pyrimidine-2(1H)-one (1) was synthesized in two steps from furan-2,3-dione and acetophenon semicarbazone reaction with loss of carbon dioxide and water, yielding the 1-methylenaminopyrimidine-2-one derivative in moderate yields. The hydrolysis of 1-methylenaminopyrimidine derivative afforded the N-aminopyrimidine-2-one derivative (1). After that, we carried out the reaction of N-aminopyrimidine-2-one derivative (1) with acetylacetone (2) yielding a imine derivative 5-(4-methoxybenzoyl)-4-(4-methoxyphenyl)-1-((4-oxopentan-2-ylidene) amino) pyrimidin-2(1H)-one (3). The general outline of the reactions studied is shown in Figure 2. In the experimental studies, the structure of the molecule was characterized by FT-IR, <sup>1</sup>H NMR and <sup>13</sup>C NMR spectroscopies. DFT and molecular docking calculations of the studied molecule were done. Afterwards, the ADME/T calculations of the molecule were done and the anti SARS-CoV-2 properties of the molecules were examined.

## Methods

### Reagent and materials

Chemicals and all solvents were commercially available and used without further purification. Melting points were determined on the digital melting point apparatus (Electrothermal 9100) and are were uncorrected. The compounds were routinely checked for their homogeneity by TLC (Thin Layer Chromatography) using DC Alufolien Kieselgel 60 F254 (Merck) and Camag TLC lamp (254/366 nm). Microanalyses were performed on a Leco CHNSO-932 Elemental Analyzer and the results agreed favorably with the calculated values. The IR spectra were recorded on a Shimadzu Model 8400 FT-IR spectrophotometer. The <sup>1</sup>H and <sup>13</sup>C NMR spectra were recorded on a Bruker 400(100) MHz Ultra Shield instrument. The chemical shifts are reported in ppm from tetramethylsilane as an internal standard and are given in δ (ppm).

### Theoretical methods

Theoretical calculations provide important information about the chemical and biological properties of molecules. Many quantum chemical parameters are obtained from theoretical calculations. The calculated parameters are used to explain the chemical activities of the molecules. Many programs are used to calculate

molecules. These programs are Gaussian09 RevD.01 (45), GaussView 6.0 (46), and Chemcraft V1.8 (47). By using these programs, calculations were done in C (50) methods with the 6-31++g(d,p) basis set. As a result of these calculations, many quantum chemical parameters have been found. Each parameter describes a different chemical property of molecules. These parameters are HOMO (Highest Occupied Molecular Orbital), LUMO (Lowest Unoccupied Molecular Orbital),  $\Delta E$  (HOMO-LUMO energy gap), chemical potential ( $\mu$ ), electrophilicity ( $\omega$ ), chemical hardness ( $\eta$ ), and global softness ( $\sigma$ ). Many parameters such as nucleophilicity ( $\epsilon$ ), dipole moment, and energy value are calculated (51, 52).

$$\chi = -\left(\frac{\partial E}{\partial N}\right)_{v(r)} = \frac{1}{2} (I + A) \cong -\frac{1}{2} (E_{HOMO} + E_{LUMO})$$

$$\eta = -\left(\frac{\partial^2 E}{\partial N^2}\right)_{v(r)} = \frac{1}{2} (I - A) \cong -\frac{1}{2} (E_{HOMO} - E_{LUMO})$$

$$\sigma = 1/\eta \quad \omega = \chi^2/2\eta \quad \epsilon = 1/\omega$$

Molecular docking calculations are performed to compare the biological activities of molecules against biological materials. The program developed by Maestro Molecular modeling platform (version 12.8) by Schrödinger (53) was used for molecular docking calculations. The Calculations were made up of several steps and each step was done differently. In the first step, the protein preparation module (54) was used in the preparation of proteins. In this module, the active sites of the proteins were determined. In the next step, the studied molecule was prepared. First, the molecule was optimized in the gaussian software program, then the LigPrep module (55) was prepared for calculations using optimized structures. The Glide ligand docking module (56) was used to examine the interactions between the molecules and the cancer protein after preparation. Calculations were done using the OPLS3e method in all calculations. Finally, ADME/T analysis were performed to examine the drug potential of the studied molecules. The Qik-prop module (57) of the Schrödinger software was used to predict the effects and reactions of molecules in human metabolism.

## Results and discussion

### Synthesis

1-Amino-5-(4-methoxybenzoyl)-4-(4-methoxyphenyl)pyrimidine-2(1H)-one 1 (0.2 g, 0.6 mmol), acetylacetone 2 (0.12 g,

**Tab. 2. Numerical values of the docking parameters of molecule against enzymes.**

	7BV1	7BUY	7QO7
Docking Score	-3.56	-2.63	-5.10
Glide ligand efficiency	-0.11	-0.08	-0.16
Glide hbond	-0.16	0.00	-0.46
Glide evdw	-30.17	-27.99	-25.29
Glide ecoul	-2.66	1.54	-7.26
Glide emodel	-26.34	-11.01	-26.26
Glide energy	-32.83	-26.44	-32.55
Glide einternal	15.09	36.40	21.34
Glide posenum	119	227	370

**Tab. 3. ADME properties of molecule.**

	Molecule	Reference Range
mol_MW	433	130–725
dipole (D)	5.4	1.0–12.5
SASA	716	300–1000
FOSA	355	0–750
FISA	138	7–330
PISA	222	0–450
WPSA	0	0–175
volume (A3)	1344	500–2000
donorHB	0	0–6
acceptHB	8.5	2.0–20.0
glob (Sphere =1)	0.8	0.75–0.95
QPpolrz (A3)	44.0	13.0–70.0
QPlogPC16	13.2	4.0–18.0
QPlogPoct	19.4	8.0–35.0
QPlogPw	10.3	4.0–45.0
QPlogPo/w	3.2	-2.0–6.5
QPlogS	-3.9	-6.5–0.5
CIQlogS	-5.4	-6.5–0.5
QPlogHERG	-5.5	*
QPPCaco (nm/sec)	488	**
QPlogBB	-1.3	-3.0–1.2
QPPMDCK (nm/sec)	228	**
QPlogKp	-2.4	Kp in cm/hr
IP (ev)	9.3	7.9–10.5
EA (eV)	1.0	-0.9–1.7
#metab	3	1–8
QPlogKhsa	-0.1	-1.5–1.5
Human Oral Absorption	3	-
Percent Human Oral Absorption	94	***
PSA	122.7	7–200
RuleOffive	0	Maximum is 4
RuleOfThree	0	Maximum is 3
Jm	0.2	-

\* concern below -5, \*\* < 25 is poor and > 500 is great, \*\*\* < 25 % is poor and > 80 % is high.

1.2 mmol) and *p*-toluenesulphonic acid catalyst were homogeneously mixed. The mixture was heated at 80 °C and kept at this temperature for 4 h without any solvent in a calcium chloride guard tube fitted round bottom flask of 50 mL. Then, the residue was treated with ether and filtered and the formed crude product 3 was recrystallized from ethanol and allowed to dry over P<sub>2</sub>O<sub>5</sub> (Fig. 2).

The structure of 3 was established and confirmed by elemental analyses and spectral data (IR, <sup>1</sup>H NMR, <sup>13</sup>C NMR). In the IR spectra of compound (3), the C=O absorption bands were found to be at  $\nu$  1712.8 and 1660.2 cm<sup>-1</sup>. Furthermore, important structural information about 3 was obtained from the <sup>1</sup>H NMR spectrum. The multiple peaks between  $\delta$  7.70–6.79 ppm are thought to represent the aromatic protons and  $\delta$  3.80–3.75 (s, 6H, 2x-OCH<sub>3</sub>), 2.65, 2.36 ppm (s, 6H, 2x-CH<sub>3</sub>). The <sup>13</sup>C NMR signals were found to be at  $\delta$  193.11 (C=O), 55.39, 55.31 (2x-OCH<sub>3</sub>) and 30.55, 15.56 ppm (2x-CH<sub>3</sub>). The aromatic carbon signals along  $\delta$  163.39–109.54 ppm were clearly observed. Finally, the elemental analysis data along with spectroscopic data confirm the structure of 3 (Fig. 3).

### Molecular docking calculations

Theoretical calculations were made to examine both the chemical and biological activity of the studied molecule. Many quantum

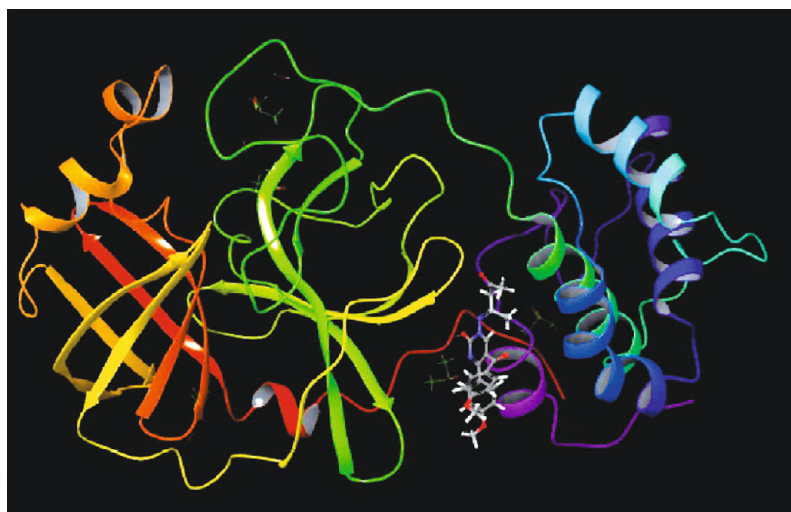
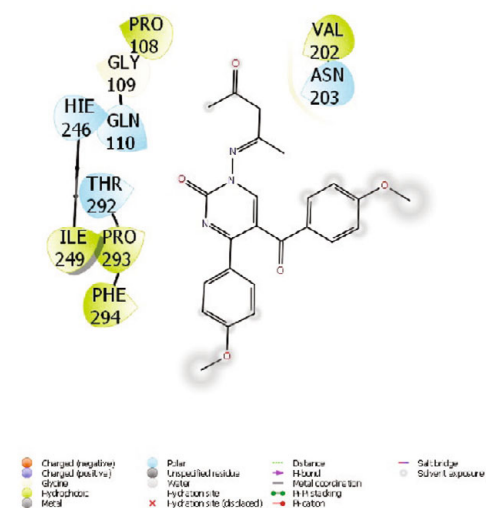


Fig. 6. Presentation of interactions of molecule with 7BUY.

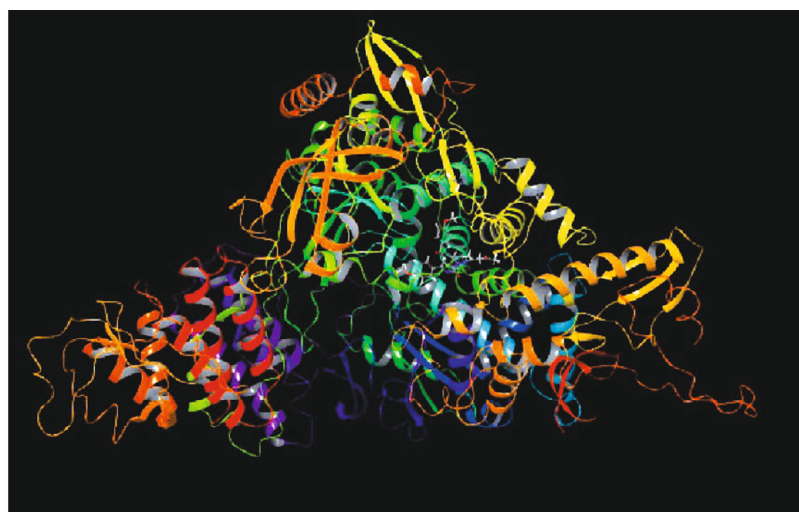
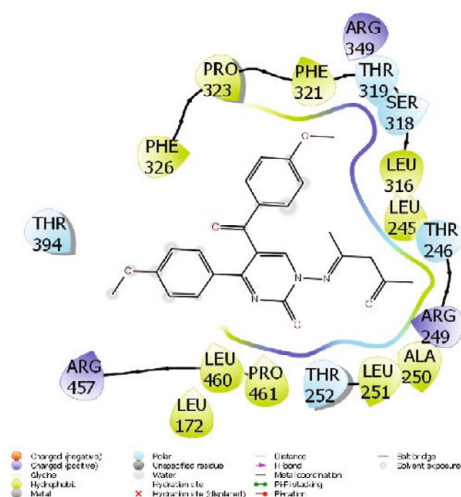


Fig. 7. Presentation of interactions of afzelin with 7BV1.

chemical parameters were calculated in the chemical activity calculations. It is possible to compare these calculations for different molecules. However, the active sites of the molecules are predicted by these calculations. Among these calculated quantum chemical parameters, two of the most important are HOMO and LUMO. These parameters are used to describe the activities of molecules. The HOMO parameter of molecules shows the ability of molecules to donate electrons and, the molecule with the most positive numerical value of this parameter has the highest activity (58–60) because the highest energy gives electrons more easily. However, another parameter used to compare the activities of molecules is LUMO. The LUMO parameter of the molecules shows the electron accepting properties of the molecules. It is seen that the molecule with the numerical value of the lower LUMO parameter has higher activity (61–63). Apart from these two parameters, the  $\Delta E$  parameter of the molecules shows the difference in the numerical values

of the HOMO and LUMO parameters of the molecules, which is the smallest molecule with the highest activity. The other calculated parameters of the molecule are given in Table 1.

The calculations of the molecule were done with 3 different methods and 3 different basis sets. It was investigated how the parameters of the molecules were affected by the calculations made in this way (Fig. 4).

Molecular docking calculations were performed to compare the activity of molecules against biological materials. In these calculations, it was tried to compare their activities against SARS-CoV 2 virus, one of the most important diseases of today. There are many receptor sites in the SARS-CoV-2 virus. A SARS-CoV-2 virus consists of various structural, nonstructural and accessory proteins that are responsible for its different functions in viral infection. There are four main structural proteins; spike (S), membrane (M), envelope (E) and nucleocapsid (N) proteins along

with 16 non-structural proteins (nsp 1-16) and accessory proteins (62). In this study, the crystal structure of RNA-dependent RNA polymerase protein from SARS-CoV-2 (PDB ID:7BV1) (64), the crystal structure of COVID-19 main protease (PDB ID:7BUY) (65), and the crystal structure of SARS-CoV-2 S Omicron Spike B.1.1.529 (PDB ID: 7QO7) (66) were investigated for interaction of the molecule and the proteins (Tab. 2)

The numerical values of all parameters obtained are given in Table 2. Among these parameters, the docking score parameter is the most important parameter and the activity of the molecule with the most negative value is the highest (61, 62, 67) (Figs 5, 6, 7).

Considering the results obtained from the molecular docking calculations, the numerical value of the docking score parameter of the molecule against the spike protein of the SARS-CoV-2 virus is -5.10. Against another protein, the main protease protein, the docking score of the molecule is -2.63. Finally, it was observed that the molecule has a docking score of 3.56 against RNA-dependent RNA polymerase protein (Tab. 3).

After molecular docking calculations, ADME/T calculations were done to examine the drug potential of the molecule. With these calculations, predictions of the movements of molecule in human tissues and cells were tried. A parameter was calculated by ADME/T analysis. In the parameters found as a result of these calculations, firstly, their chemical properties were examined, and then the parameters that examined the effects and reactions in human tissues and cells were calculated. The most important parameters that determine whether this molecule can be a drug are the RuleOfFive (68, 69) and RuleOfThree (70) parameters, the numerical value of which is required to be zero.

## Conclusions

In this study, a new compound (3) was synthesized from the condensation reaction of N-amino-pyrimidine-2-one derivative (1) with 1,3-dicarbonyl compound. The mechanistic proposal for the formation of 3 is given in Figure 3. The structure of the newly synthesized compound 3 was determined by the FT-IR, <sup>1</sup>H and <sup>13</sup>C NMR spectroscopic data and elemental analysis. Molecular docking calculations were performed to evaluate the activity of the molecule against the SARS-CoV-2 virus. Considering the obtained values, the activities of the molecule against SARS-CoV-2 RNA-dependent RNA polymerase protein, SARS-CoV-2 main protease, and SARS-CoV-2 S Omicron Spike B.1.1.529 were investigated. Its use as a drug against the SARS-CoV-2 virus was theoretically investigated with ADME/T calculations. It was seen that the numerical values of the calculated parameters are in the desired ranges. In light of these results, it will be an important guide for future in vitro and in vivo experiments.

## References

1. Gorbalenya AE, Baker SC, Baric RS, de Groot RJ, Drosten C, Gulyaeva AA et al. The species Severe acute respiratory syndrome-related coronavirus: classifying 2019-nCoV and naming it SARS-CoV-2. *Nat Microbiol* 2020; 5 (4): 536–544.

2. Wong G, Bi YH, Wang QH, Chen XW, Zhang ZG, Yao YG. Zoonotic origins of human coronavirus 2019 (HCoV-19/SARS-CoV-2): why is this work important? *Zool Res* 2020; 41 (3): 213–219.

3. Yu WB, Tang GD, Zhang L, Corlett RT. Decoding the evolution and transmissions of the novel pneumonia coronavirus (SARS-CoV-2 / HCoV-19) using whole genomic data. *Zool Res* 2020; 41 (3): 247–257.

4. Fang SY, Li KL, Shen JK, Liu S, Liu JL, Yang L et al. GESS: a database of global evaluation of SARS-CoV-2/hCoV-19 sequences. *Nucleic Acids Res* 2021; 49 (D1): D706–D714.

5. Wawrzyniak A, Kuczborska K, Lipinska-Opalka A, Bedzichowska A, Kalicki B. The 2019 novel coronavirus (2019-nCoV) – transmission, symptoms and treatment. *Pediatr Med Rodz* 2019; 15 (4): C1–C5.

6. Liu P, Tan XZ. 2019 Novel Coronavirus (2019-nCoV) Pneumonia. *Radiology* 2020; 295 (1): 19.

7. Duarte R, Furtado I, Sousa L, Carvalho C. The 2019 Novel Coronavirus (2019-nCoV): Novel Virus, Old Challenges. *Acta Medica Port* 2020; 33 (3): 155–157.

8. Chiappelli F. 2019-nCoV – Towards a 4th generation vaccine. *Bioinformation* 2020; 16 (2): 139–144.

9. WHO. WHO Director-General's opening remarks at the media briefing on COVID-19. <https://www.who.int/director-general/speeches/detail/who-director-general-s-opening-remarks-at-the-media-briefing-on-covid-19---11-march-2020> 2020.

10. WHO. Archived: WHO Timeline - COVID-19 <https://www.who.int/news/item/27-04-2020-who-timeline---covid-19> 2020.

11. Ralph R, Lew J, Zeng TS, Francis M, Xue B, Roux M et al. 2019-nCoV (Wuhan virus), a novel Coronavirus: human-to-human transmission, travel-related cases, and vaccine readiness. *J Infect Dev Countr* 2020; 14 (1): 3.

12. Li CY, Ji F, Wang L, Wang LP, Hao JG, Dai MJ et al. Asymptomatic and Human-to-Human Transmission of SARS-CoV-2 in a 2-Family Cluster, Xuzhou, China. *Emerg Infect Dis* 2020; 26 (7): 1626–1628.

13. Wang DX, Wang YQ, Sun WY, Zhang L, Ji JK, Zhang ZY et al. Population Bottlenecks and Intra-host Evolution During Human-to-Human Transmission of SARS-CoV-2. *Front Med-Lausanne* 2021; 8.

14. Cyranoski D. Mystery Deepens over Animal Source of Coronavirus. *Nature* 2020; 579 (7797): 18–19.

15. WHO. Tracking SARS-CoV-2 variants. <https://www.who.int/en/activities/tracking-SARS-CoV-2-variants/>.

16. WHO. WHO Coronavirus (COVID-19) Dashboard. <https://covid19.who.int/> 2022.

17. El-Said WA, Al-Bogami AS, Alshitari W. Synthesis of gold nanoparticles@reduced porous graphene-modified ITO electrode for spectroelectrochemical detection of SARS-CoV-2 spike protein. *Spectrochim Acta A* 2022; 264.

18. Emary KRW, Golubchik T, Aley PK, Ariani CV, Angus B, Bibi S et al. Efficacy of ChAdOx1 nCoV-19 (AZD1222) vaccine against SARS-CoV-2 variant of concern 202012/01 (B.1.1.7): an exploratory analysis of a randomised controlled trial. *Lancet* 2021; 397 (10282): 1351–1362.

19. Wall EC, Wu M, Harvey R, Kelly G, Warchal S, Sawyer C et al. AZD1222-induced neutralising antibody activity against SARS-CoV-2 Delta VOC. *Lancet* 2021; 398 (10296): 207–209.

20. Haas EJ, Angulo FJ, McLaughlin JM, Anis E, Singer SR, Khan F et al. Impact and effectiveness of mRNA BNT162b2 vaccine against SARS-

CoV-2 infections and COVID-19 cases, hospitalisations, and deaths following a nationwide vaccination campaign in Israel: an observational study using national surveillance data. *Lancet* 2021; 397 (10287): 1819–1829.

**21. Ishmatov A.** SARS-CoV-2 is transmitted by particulate air pollution: Misinterpretations of statistical data, skewed citation practices, and misuse of specific terminology spreading the misconception. *Environ Res* 2022; 204.

**22. Tuzun B, Bhawsar J.** Quantum chemical study of thiazole derivatives as corrosion inhibitors based on density functional theory. *Arab J Chem* 2021; 14 (2).

**23. Koc E, Ungordu A, Candan F.** Antioxidant properties of methanolic extract of 'Veronica multifida' and DFT and HF analyses of its the major flavonoid component. *J Mol Struct* 2019; 1197: 436–442.

**24. Tuzun B, Saripinar E.** Molecular docking and 4D-QSAR model of methanone derivatives by electron conformational-genetic algorithm method. *J Iran Chem Soc* 2020; 17 (5): 985–1000.

**25. Khalilov AN, Tüzün B, Taslimi P, Tas A, Tuncbilek Z, Keklikcioglu NC.** Cytotoxic effect, spectroscopy, DFT, enzyme inhibition, and molecular docking studies of some novel mesitylaminoopropanols: Antidiabetic and anticholinergics and anticancer potentials. *J Mol Liq* 2021; 344 (117761).

**26. Bilgili AT, Kandemir T, Tuzun B, Ariduru R, Gungel A, Abak C et al.** Octa-substituted Zinc (II), Cu (II), and Co (II) phthalocyanines with 1-(4-hydroxyphenyl)propane-1-one: Synthesis, sensitive protonation behaviors, Ag (I) induced H-type aggregation properties, antibacterial-antioxidant activity, and molecular docking studies. *Appl Organomet Chem* 2021; 35 (10).

**27. Durmaz N, Onal Z, Altural B.** Reactions of 4-benzoyl-5-[(E)-2-phenyl-1-ethenyl]-2,3-dihydro-2,3-furandione with aromatic aminonucleophiles. *Asian J Chem* 2006; 18 (2): 1261–1266.

**28. Onal Z, Daylan AC.** Reactions of 1-Amino-5-benzoyl-4-phenyl-1H-pyrimidine derivatives with various isothiocyanates. *Asian J Chem* 2007; 19 (4): 2647–2653.

**29. Onal Z, Yildirim I, Kandemirli F, Arslan T.** Experimental and theoretical studies on the reactions of 1-amino-5-benzoyl-4-phenyl-1H-pyrimidine-2-one/-thione compounds with ethyl acetoacetate. *Struct Chem* 2010; 21 (4): 809–816.

**30. Önal Z, Altural B.** Reactions of N-aminopyrimidine derivatives with 1,3-dicarbonyl compounds. *Turkish Journal of Chemistry* 1997; 23: 403–405.

**31. Onal Z, Ceran H, Sahin E.** Synthesis of Novel Dihydropyrazolo[1,5-C]Pyrimidin-7 (3h)-One/-Thione Derivatives. *Heterocycl Commun* 2008; 14 (4): 245–250.

**32. Aslan G, Onal Z.** Novel metal complexes, their spectrophotometric and QSAR studies. *Med Chem Res* 2014; 23 (5): 2596–2607.

**33. Kokbudak Z, Asian HG, Akkoc S.** New Schiff Bases Based on 1-Aminopyrimidin-2- (1h)-One: Design, Synthesis, Characterization and Theoretical Calculations. *Heterocycles* 2020; 100 (3): 440–449.

**34. Aslan HG, Akkoc S, Kokbudak Z.** Anticancer activities of various new metal complexes prepared from a Schiff base on A549 cell line. *Inorg Chem Commun* 2020; 111.

**35. Kokbudak Z, Saracoglu M, Akkoc S, Cimen Z, Yilmazer MI, Kandemirli F.** Synthesis, cytotoxic activity and quantum chemical calculations of new 7-thioxopyrazolo[1,5-f]pyrimidin-2-one derivatives. *J Mol Struct* 2020; 1202.

**36. Saracoglu M, Kokbudak Z, Yalcin E, Kandemirli F.** Synthesis and DFT Quantum Chemical Calculations of 2-Oxopyrimidin-1 (2H)-yl-Urea and Thiorea Derivatives. *J Chem Soc Pakistan* 2019; 41 (5): 841–858.

**37. Saracoglu M, Kokbudak Z, Cimen Z, Kandemirli F.** Synthesis and DFT Quantum Chemical Calculations of Novel Pyrazolo[1,5-c]pyrimidin-7 (1H)-one Derivatives. *J Chem Soc Pakistan* 2019; 41 (3): 479–488.

**38. Gondkar AS, Deshmukh VK, Chaudhari SR.** Synthesis, characterization and in vitro anti-inflammatory activity of some substituted 1,2,3,4 tetrahydropyrimidine derivatives. *Drug Invention Today* 2013; 5: 175–181.

**39. Ma LY, Pang LP, Wang B, Zhang M, Hu B, Xue DQ et al.** Design and synthesis of novel 1,2,3-triazole-pyrimidine hybrids as potential anticancer agents. *Eur J Med Chem* 2014; 86: 368–380.

**40. Ramiz MMM, El-Sayed WA, El-Tantawy AI, Abdel-Rahman AAH.** Antimicrobial Activity of New 4,6-Disubstituted Pyrimidine, Pyrazoline, and Pyran Derivatives. *Arch Pharm Res* 2010; 33 (5): 647–654.

**41. Rai D, Chen WM, Tian Y, Chen XW, Zhan P, De Clercq E et al.** Design, synthesis and biological evaluation of 3-benzyloxy-linked pyrimidinylphenylamine derivatives as potent HIV-1 NNRTIs. *Bioorgan Med Chem* 2013; 21 (23): 7398–7405.

**42. Panahi F, Yousefi R, Mehraban MH, Khalafi-Nezhad A.** Synthesis of new pyrimidine-fused derivatives as potent and selective antidiabetic alpha-glucosidase inhibitors. *Carbohydr Res* 2013; 380: 81–91.

**43. Perspicace E, Jouan-Hureaux V, Ragno R, Ballante F, Sartini S, La Motta C et al.** Design, synthesis and biological evaluation of new classes of thieno [3,2-d]pyrimidinone and thieno[1,2,3]triazine as inhibitor of vascular endothelial growth factor receptor-2 (VEGFR-2). *Eur J Med Chem* 2013; 63: 765–781.

**44. Chikhale R, Menghani S, Babu R, Bansode R, Bhargavi G, Karodia N et al.** Development of selective DprE1 inhibitors: Design, synthesis, crystal structure and antitubercular activity of benzothiazolylpyrimidine-5-carboxamides. *Eur J Med Chem* 2015; 96: 30–46.

**45. M.J. F, G.W. T, H.B. S, G.E. S, M.A. R, J.R. C et al.** Gaussian 09, revision D.01. Gaussian Inc, Wallingford CT 2009.

**46. Dennington R, Keith TA, Millam JM.** GaussView 6.0. 16, Shawnee Mission 2016.

**47. Zhurko GA, & Zhurko DA.** ChemCraft, version 1.6. URL: <http://www.chemcraftprog.com> 2009.

**48. Becke AD.** Density-Functional Thermochemistry .3. The Role of Exact Exchange. *J Chem Phys* 1993; 98 (7): 5648–5652.

**49. Vautherin D, & Brink DM.** Hartree-Fock calculations with Skyrme's interaction. I. Spherical nuclei. *Phys Rev C* 1972; 5: 626–647.

**50. Hohenstein EG, Chill ST, Sherrill CD.** Assessment of the Performance of the M05-2X and M06-2X Exchange-Correlation Functionals for Noncovalent Interactions in Biomolecules. *J Chem Theory Comput* 2008; 4 (12): 1996–2000.

**51. Gungel A, Bilgili AT, Piskin H, Tuzun B, Delibas NC, Yarasir MN et al.** Comparison of spectroscopic, electronic, theoretical, optical and surface morphological properties of functional manganese (III) phthalocyanine compounds for various conditions. *J Mol Struct* 2019; 1193: 247–264.

**52. Gungel A, Bilgili AT, Piskin H, Tuzun B, Yarasir MN, Gunduz B.** Optoelectronic parameters of peripherally tetra-substituted copper (ii) phthalocyanines and fabrication of a photoconductive diode for various conditions. *New J Chem* 2020; 44 (2): 369–380.

53. Schrödinger Release 2021-3: Maestro, Schrödinger, LLC, New York, NY, 2021.
54. Schrödinger Release 2019-4: Protein Preparation Wizard; Epik, Schrödinger, LLC, New York, NY, 2016; Impact, Schrödinger, LLC, New York, NY, 2016; Prime, Schrödinger, LLC, New York, NY, 2019.
55. Schrödinger Release 2021-3: LigPrep, Schrödinger, LLC, New York, NY, 2021.
56. Aktas A, Tuzun B, Aslan R, Sayin K, Ataseven H. New anti-viral drugs for the treatment of COVID-19 instead of favipiravir. *J Biomol Struct Dyn* 2021; 39 (18): 7263–7273.
57. Schrödinger Release 2021-3: QikProp, Schrödinger, LLC, New York, NY, 2021.
58. Aktas A, Tuzun B, Kafa AHT, Sayin K, Ataseven H. How do arbidol and its analogs inhibit the SARS-CoV-2? *Bratisl Med J* 2020; 121 (10): 705–711.
59. Taslimi P, Demir Y, Duran HE, Koçyiğit ÜM, Tüzün B, Aslan ON et al. Some old 2- (4- (Aryl)-thiazole-2-yl)-3a, 4, 7, 7a-tetrahydro-1H-4, 7-tethanoisindole-1, 3 (2H)-dione derivatives: Synthesis, inhibition effects and molecular docking studies on Aldose reductase and  $\alpha$ -Glycosidase. *Cumhuriyet Science Journal* 2021; 42: 553–564.
60. Riaz MT, Yaqub M, Shafiq Z, Ashraf A, Khalid M, Taslimi P et al. Synthesis, biological activity and docking calculations of bis-naphthoquinone derivatives from Lawsonia. *Bioorg Chem* 2021; 114.
61. Bilgili AT, Bilgili HG, Hepokur C, Tuzun B, Günsel A, Zengin M et al. Synthesis of (4R)-2- (3-hydroxyphenyl)thiazolidine-4-carboxylic acid substituted phthalocyanines: Anticancer activity on different cancer cell lines and molecular docking studies. *Appl Organomet Chem* 2021; 35 (7).
62. Erdogan M, Taslimi P, Tuzun B. Synthesis and docking calculations of tetrafluoronaphthalene derivatives and their inhibition profiles against some metabolic enzymes. *Arch Pharm* 2021; 354 (6).
63. Poustforoosh A, Hashemipour H, Tuzun B, Pardakhty A, Mehra-bani M, Nematollahi MH. Evaluation of potential anti-RNA-dependent RNA polymerase (RdRP) drugs against the newly emerged model of COVID-19 RdRP using computational methods. *Biophys Chem* 2021; 272.
64. Yin WC, Mao CY, Luan XD, Shen DD, Shen QY, Su HX et al. Structural basis for inhibition of the RNA-dependent RNA polymerase from SARS-CoV-2 by remdesivir. *Science* 2020; 368 (6498): 14997.
65. Jin ZM, Zhao Y, Sun Y, Zhang B, Wang HF, Wu Y et al. Structural basis for the inhibition of SARS-CoV-2 main protease by antineoplastic drug carmofur. *Nat Struct Mol Biol* 2020; 27 (6): 529.
66. Herrera NG, Morano NC, Celikgil A, Georgiev GI, Malonis RJ, Lee JH et al. Characterization of the SARS-CoV-2 S Protein: Biophysical, Biochemical, Structural, and Antigenic Analysis. *ACS Omega* 2021; 6 (1): 85–102.
67. Tokali FS, Taslimi P, Demirciolu IH, Sendil K, Tuzun B, Gulcin I. Novel phenolic Mannich base derivatives: synthesis, bioactivity, molecular docking, and ADME-Tox Studies. *J Iran Chem Soc* 2021.
68. Lipinski CA, Lombardo F, Dominy BW, Feeney PJ. Experimental and computational approaches to estimate solubility and permeability in drug discovery and development settings. *Adv Drug Deliver Rev* 1997; 23 (1–3): 3–25.
69. Lipinski CA. Lead- and drug-like compounds: the rule-of-five revolution. *Drug Discov Today Technol* 2004; 1 (4): 337–341.
70. Jorgensen WL, Duffy EM. Prediction of drug solubility from structure. *Adv Drug Deliver Rev* 2002; 54 (3): 355–366.

Received January 6, 2022.  
Accepted February 21, 2022.